

Theoretical Insights into the Carbon Linker Length Effects on the Radical Scavenging Activity of Curcumin

Lusia S. P. Boli^a, Febdian Rusydi^{b,c*}, Vera Khoirunisa^d, Adhitya Gandaryus Saputro^{a,e}, Muhammad Haris Mahyuddin^{a,e}, Kazunari Yoshizawa^f, Heni Rachmawati^{e,g}, Hermawan K. Dipojono^{a,e*}

^aAdvanced Functional Materials Research Group, Faculty of Industrial Technology, Institut Teknologi Bandung, Bandung 40132, Indonesia; ^bDepartment of Physics, Faculty of Science and Technology, Universitas Airlangga, Surabaya 60115, Indonesia; ^cResearch Center for Quantum Engineering Design, Faculty of Science and Technology, Universitas Airlangga, Surabaya 60115, Indonesia; ^dDepartment of Engineering Physics, Institut Teknologi Sumatera, Lampung Selatan 35365, Indonesia; ^eResearch Center for Nanosciences and Nanotechnology, Institut Teknologi Bandung, Bandung 40132, Indonesia; ^fInstitute for Materials Chemistry and Engineering, Kyushu University, Fukuoka 819-0395, Japan; ^gSchool of Pharmacy, Institut Teknologi Bandung, Bandung 40132, Indonesia

Abstract Linker length is one crucial factor affecting the free radical scavenging activity of curcumin. However, identifying an optimal linker length that maintains the desired activity remains challenging. This study offers a thermodynamic evaluation of the influence of linker length on free radical scavenging activity of curcumin, specifically through the hydrogen atom transfer mechanism, in water solvents. Our first-principles calculations reveal that both elongating and shortening the linker promotes a more favorable hydrogen atom transfer at the phenolic O—H and the C—H bond within the linker, respectively. Therefore, linker length should be considered in developing curcumin as a multifunctional medicine.

Keywords: Curcumin linker length; first-principles calculations; multifunctional medicine; radical scavenging activity.

Introduction

Research in the medicinal chemistry focuses on the free radical scavenging activity of curcumin, as this activity benefits human health. One of the early reports on the scavenging activity of curcumin was published in 1972 by Sharma *et al.* [1] The report highlighted curcumin's ability to inhibit *in vitro* lipid peroxidation. One key radical that promotes lipid peroxidation is the highly reactive peroxy radicals [2, 3]. Numerous studies demonstrate curcumin's effectiveness in scavenging these radicals [4–7]. This scavenging ability positions curcumin as a potential therapeutic agent for various diseases related to free radicals, including spinal cord injury [8,9], cataract [10], neurodegenerative disorders [11,12], cancer [13,14], and diabetes [15,16].

Enhancing the free radical scavenging activity of curcumin can be achieved through experimental and computational studies. The studies focus on structural modifications of the aromatic rings — containing *o*-methoxy and phenolic O—H — and carbon linker — containing β -diketone moiety (See Figure 1a). Modifying the aromatic rings involves maintaining or adding phenolic O—H groups and maintaining or replacing *o*-methoxy groups with other electron donor groups [17–21]. Previous studies suggested the phenolic O—H groups as active sites of curcumin [21]. On the other hand, the *o*-methoxy groups facilitate

***For correspondence:**
rusydi@fst.unair.ac.id

Received: 25 Oct. 2023

Accepted: 11 Dec. 2023

©Copyright Boli. This article is distributed under the terms of the [Creative Commons Attribution License](#), which permits unrestricted use and redistribution provided that the original author and source are credited.

hydrogen atom transfer from the phenolic O—H [22,23]. Modifying the carbon linker includes replacing the β -diketone moiety, introducing a cyclic structure, and eliminating double bonds [18,24–26]. Curcumin analogs without double bonds in the linker exhibit enhanced scavenging activity toward peroxy radicals. Both experimental and computational studies agreed that the scavenging of peroxy radicals occurs through hydrogen atom transfer mechanism [27–29], since the insolubility of curcumin in water may limit electron transfer mechanism [30]. On the other hand, the presence of β -diketone moiety in the linker enables keto-enol tautomerism, with the keto form (Figure 1b) being dominant in water solvents [31,32]. Sun *et al.* suggested both enol and keto forms are involved in hydrogen atom transfer mechanism [33].

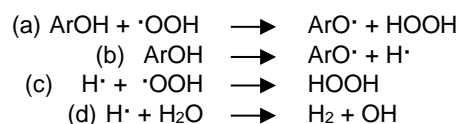
Although it is known that enhancing the free radical scavenging activity of curcumin is attainable by finding an optimal linker length, several problems remain. One fundamental problem is determining the optimal linker length that maintains the desired scavenging activity. Previously, despite discrepancies in their findings, Shang *et al.* [26] and Li *et al.* [34] observed the effect of linker length on the scavenging activity. Their observations were limited to curcumin with a seven-carbon linker and its monocarbonyl analog with a five-carbon linker. Hence, a study that provides a broader relationship for the fundamental problem is needed. To evaluate the effect of linker length on the free radical scavenging activity, we determined the correlation between linker length and the thermochemistry of hydroperoxyl radical scavenging reaction using first-principles calculations. Our study included twelve molecules with linker lengths ranging from three to nine carbon atoms in water solvents.

This paper reports the correlation between curcumin linker length and an X-H bond dissociation energies (and the Gibbs free energies of scavenging reaction). It begins by modeling hydroperoxyl radical scavenging reactions using hydrogen atom transfer, designing twelve molecules grouped into three series, and modeling the water solvent with Polarizable Continuum Model (PCM) using first-principles calculations. The results and discussion are divided into topics of the ground state structures, the bond dissociation energies, and the Gibbs free energy of reactions. Finally, the paper highlights the effects of the linker length in the hydrogen atom transfer based on the thermochemistry point of view. This highlight, in turn, will provide insight into the factors contributing to enhancing the scavenging activity for medicinal applications.

Materials and Methods

Reaction and Molecular Models

Reaction (a) in Scheme 1 models the scavenging of hydroperoxyl radical ($\cdot\text{OOH}$) by phenolic antioxidants (ArOH) using the one-step hydrogen atom transfer (HAT) mechanism. We chose hydroperoxyl radical because it was the simplest form of peroxy radicals. Like other peroxy radicals, it also involves in lipid peroxidation [35, 36]. Since experimental and computational evidences showed that the scavenging of peroxy radicals by ArOH occurred through HAT [27–29], we chose this mechanism in this study.



Scheme 1: The reactions of interest.

In this study, the ArOH were two forms of curcumin and their 10 analogs. The two forms of curcumin and their analogs were constructed in three series based on the structures in Figure 1. Each series was differentiated by the type of moiety/group in the linker. Table 1 contains a complete list of all members in each series. Series I, with an enol moiety (the OH—3—4—5—O in Figure 1a), was curcumin analogs [Ia(n=3), Ib(n=5), and Id(n=9)] and the enol form of curcumin [Ic(n=7)]; series II, with a keto moiety (the O—3—4—5—O in Figure 1b), was dicarbonyl analogs [IIa(n=3), IIb(n=5), and IIc(n=9)] and the keto form of curcumin [IIc(n=7)]; series III, with a carbonyl group (the O—4 in Figure 1c), were monocarbonyl analogs.

There were different reasons to choose each series. Series I and II were selected because enol and keto tautomers are present in water solvents. Series III was included to address the issue discussed in paragraph 3 of Introduction. We assumed that the geometries of each series are symmetric and that the possible active sites (1, 2, and 3 in Figure 1) in the left and right halves of the three series have similar characteristics.

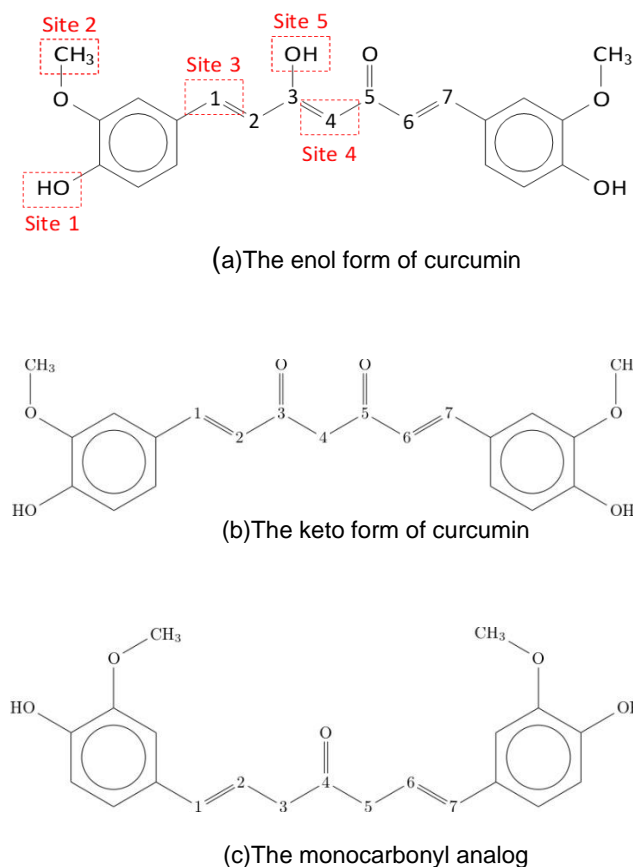


Figure 1. The basic structures to design the three series of curcumin and its analogs. The enol form was taken from the observation of Sanphui *et al.* [58]. and used as a template. Number 1-7 represents carbon atoms in the linker (n). The analogs were designed by either adding or subtracting the number of carbon atoms. The red boxes mark the location of possible active sites.

Table 1. List of the members of the three series of curcumin and its analogs based on the number of carbon atoms in the linker (n)

No.	Series I	Series II	Series III	n
1.	Ia	IIa	IIIa	3
2.	Ib	IIb	IIIb	5
3.	Ic	IIc	IIIc	7
4.	Id	IIId	IIId	9

Solvent Models

We employed the PCM [37] to model a water solvent, which represents the biological environment where radical scavenging reactions occur. In a water solvent, Reaction (c) in Scheme 1 competes with Reaction (d) in Scheme 1. In the gas phase, experimental observation showed that both reactions were exothermic and endothermic, respectively [38, 39]. This observation suggested the former is more favorable. To ensure PCM can effectively model a water solvent, we calculated the enthalpy of reactions for both reactions without and with PCM (Table S1). Our results aligned with the experimental results, indicating that PCM is appropriate to model the water solvent in this research. In addition, previously, PCM has been able to explain experimental results regarding the antioxidant activity of oleuropein and its derivatives [40].

Reaction Energy Calculations

We used two thermochemical quantities to evaluate the correlation between linker length and the $\cdot\text{OOH}$ scavenging reactions. They were bond dissociation energies (BDE), $\Delta_r H^\circ$, and the Gibbs free energies of HAT, $\Delta_r G^\circ$. The bond dissociation energy is calculated according to Equation 1 and based on Reaction

(b) in Scheme 1. On the other hand, the $\Delta_r G^\circ$ is calculated according to Equation 2 and based on Reaction (a) in Scheme 1.

$$\Delta_r H^\circ = [H^\circ(\text{ArO}\bullet) + H^\circ(\text{H}\bullet)] - [H^\circ(\text{ArOH})] \quad (1)$$

$$\Delta_r G^\circ = [G^\circ(\text{ArO}\bullet) + G^\circ(\text{HOOH})] - [G^\circ(\text{ArOH}) + G^\circ(\bullet\text{OOH})] \quad (2)$$

In a scavenging reaction, a hydrogen atom is dissociated from the ArOH before it reacts with OOH. According to the Bell-Evans-Polanyi principle, there is a linear relationship between the dissociation energy and the activation energy of an O–H or C–H bond dissociations [41]. Therefore, the dissociation energy can be an indicator of scavenging activity, as suggested by Wright *et al* [42].

As a benchmark, we used the dissociation energy of the O–H bond of phenol. In the gas phase, our calculated dissociation energy of the O–H bond of phenol is 88.32 kcal/mol. This value fits perfectly in the range of experimental values (87.36 - 88.60 kcal/mol) [43].

Computational Details

This work uses first-principles calculations, which is density-functional calculations [44, 45] integrated into Gaussian 16 [46] software. The calculations have been used for studying homolytic bond dissociation [47, 48] and chemical reactions [49, 50]. For performing the calculations, we used M06-2X and 6-311++G(d,p) as the exchange-correlation (XC) functional and basis set (BS), respectively. Developer M06-2X suggested it for thermochemical calculations [51]. We have used the XC for modeling an O–H and C–H bond dissociations previously [52, 53]. Other researchers also used the XC to study other chemical reactions [54].

We performed geometry optimization and vibrational frequency calculations. The optimizations obtained singlet-spin states for ArOH and doublet-spin states for $\bullet\text{OOH}$ and ArO \bullet in Reaction 1. The vibrational frequency calculations were performed to obtain thermal correction at room temperature (298.15 K). We followed the calculation routines in Ref. [55]. The calculation in a water solvent used PCM implemented in Gaussian 16 software. From both routines, we obtained (1) the sum of electronic and thermal enthalpies $[(\epsilon_0 + H_{corr})_{\text{ArO}\bullet}]$ and (2) the sum of electronic and thermal free energies $[(\epsilon_0 + G_{corr})_{\text{ArO}\bullet}]$ at the standard temperature and pressure. $(\epsilon_0 + H_{corr})_{\text{ArO}\bullet}$ and $(\epsilon_0 + G_{corr})_{\text{ArO}\bullet}$ were $H^\circ(\text{ArO}\bullet)$ and $G^\circ(\text{ArO}\bullet)$ in equation (1) and (2), respectively. Lastly, Natural Bond Orbital (NBO) calculations were performed to determine the orbital hybridization [56, 57].

Results and Discussion

The Ground State Structures

The linker elongation affected the planarity of the three series of curcumin and its analogs in different ways. The planarity of series I alternated between planar and non-planar as the linker elongated (Figure 2a to 2d), while the planarity of series III alternated inversely (Figure S1e to S1h). On the other hand, all the analogs in series II exhibited a non-planar configuration (Figure S1a to S1d). The planarity of Ic (Figure 2c) was consistent with the previous observation [58], while the planarity of Ilc (Figure S1c) aligned with the calculations reported by Benassi *et al.* [59]. Table S3 presents the calculated bond lengths for these structures.

Most members of the three series were not planar because conjugated systems were absent in their linkers. The non-planarity was evident in (1) the twisting of the linker of Id (Figure 2d), IId (Figure S1d), and IIIc (Figure S1g), (2) the folding of the linker of Ib (Figure 2b), IIb (Figure S1b) and IIIa (Figure S1e), and (3) the folding of the methylene group in series II (Figure S1a to S1d). We note that the twisting and folding of the linker occurred as the linker elongated or shortened. The data on bonding orbitals in Table S4 show that in areas where the twisting and folding occurred, there was no conjugated system. For example, in parameters 5–10 (Ib(n=5)), there were no alternating single C–C and double C=C bonds.

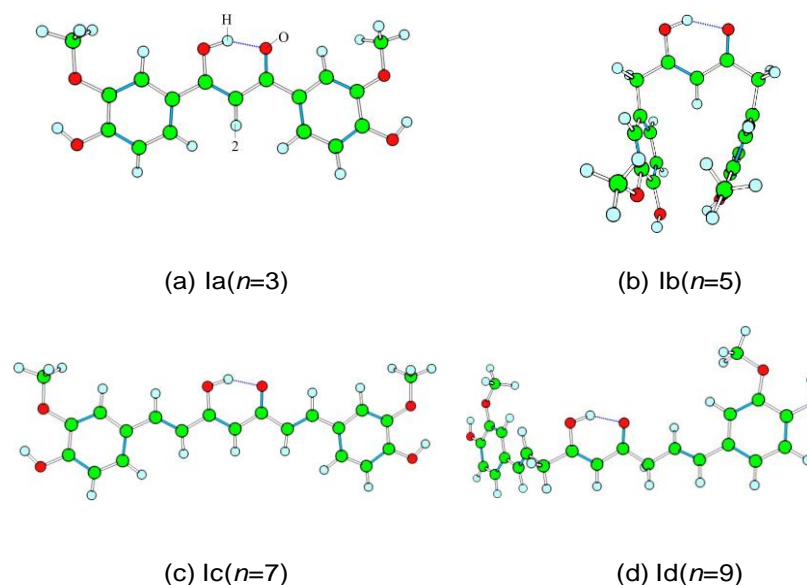


Figure 2. Optimized geometries of all members of series I. The optimized geometries of series II and III are shown in Figure S1. All the Cartesian coordinates are shown in Table S2. Atom numbering is shown in Figure 1

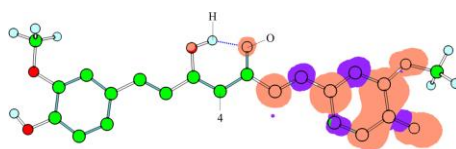
The Bond Dissociation Energies

The phenolic O—H bond in curcumin Radical spin delocalization influenced the phenolic O—H (site 1) dissociation energy. The dissociation energy of site 1 in Ic and IIc were the lowest compared to the other sites (see Figures 4a and 4b). The energy was also lower than the dissociation energy of the phenolic O—H in phenol (87.74 kcal/mol). Dissociation of site 1 lead to the formation of a phenoxyl radical with a highly delocalized unpaired electron (Figure 3). These results support the conclusion of Brinck *et al.* [60] that delocalization is the dominant factor determining the dissociation energy of phenolic O—H in phenol. Therefore, the hydrogen atom transfer of the phenolic O—H in curcumin is the easiest, consistent with experimental [4, 29, 61, 62] and computational [29, 63] studies.

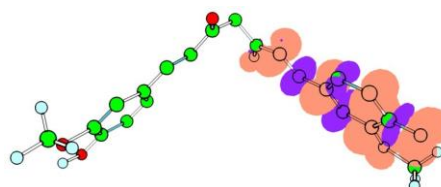
The effect of the moieties in the linker The type of moieties in the linker only affected the dissociation energy of the C—H bond (site 4) within the moieties. The average dissociation energy of site 4 in series II was 22.30 kcal/mol lower than that in series I. This value was much greater than the mean unsigned error (MUE) of M06-2X — 1.2 kcal/mol for the homolytic bond dissociation energies [64]. These results indicate the HAT of the methylene group in the β -diketones of series II is easier than the HAT of the same group in series I. The results are in accordance with the suggestion of Sugiyama *et al.* [65] that the β -diketone group exhibits antioxidant activity.

The effect of the linker length Linker elongation, by increasing the value of n , weakened the phenolic O—H bond (site 1) of the three series gradually (Figure 4). This weakening could be seen from the decrease in site 1 dissociation energy as the value of n increased. Most of this decrease, between 1.96–4.64 kcal/mol, was greater than the MUE. Therefore, this weakening is significant.

The weakening of the phenolic O—H bond was due to the increased stability of the phenoxyl radical. As n increased, oxygen atoms, which lose hydrogen atoms, became more negative (Table S5). Therefore, the Coulombic attraction between those oxygen atoms and the hydrogen atoms in the methoxy group increases. As a result, the stability of the phenoxyl radical increased. These results complement the results obtained by de Heer *et al.* [22], Chen *et al.* [23] and Somparn *et al.* [18] In addition to the hydrogen bonding between the methoxy and phenolic O—H groups, they suggested, the stability of the phenoxyl radical plays a role in weakening the phenolic O—H bond. Thus, hydrogen atom transfer from the phenolic O—H occurs.



(a) Phenoxyl radical of the enol form of curcumin [Ic($n=7$)]



(b) Phenoxyl radical of the keto form of curcumin [IIc($n=7$)]

Figure 3. Spin density of phenoxyl radicals with isosurface value of 0.002. Some hydrogen atoms are omitted for clarity. Orange and purple colors represent alpha- and beta- electron densities, respectively. Atom numbering is shown in Figure 1. The spin densities of other radicals are shown in Figure S2

Instead of phenolic O—H, linker shortening weakened the C—H bond in the linker and the O—H bond in the β -diketone moiety significantly (Figure 4). As the value of n decreased, the dissociation energies of the C—H bond (site 3) of Ib, IIb and IIIa and the O—H bond (site 5) of Ib decreased in the range of 16–22 kcal/mol. This significant decrease caused the dissociation energy of site 3 to be similar to or even lower than that of site 1. However, it was not the case for site 5. Therefore, the C—H bond in the linker can easily transfer its hydrogen atoms as easily as phenolic O—H.

The role of a conjugated system The absence of a conjugated system in the linker directly affected the strength of the C—H bond in the linker. This was evident in molecules Ib($n=5$), IIb($n=5$), and IIIa($n=3$), where two specific conditions indicated a reduced strength of the C—H bond. These conditions were the presence of a hybrid sp^λ with λ greater than three (see highlighted cells in Table S6) and the formation of a stable radical (marked in red in Figure S3) due to delocalized unpaired electrons (Figure S4a, S4d, and S4g).

On the other hand, the absence of a conjugated system in the linker indirectly affected the dissociation energy of the O—H bond in the moiety. This was demonstrated in the folded structure of the linker Ib ($n=5$), which gave rise to three distinct conditions. These conditions were the weakest coulomb attraction between the positively charged H atom (in the O—H bond) and the negatively charged O atom (in the C—O bond near the O—H bond) due to their largest distance (Table S7), the largest magnitude of the O—HO angle (Table S7), and the highest frequency of O—H vibrations with the lowest intensity (red line in Figure S5). The last condition aligns with the IUPAC criterion of weaker hydrogen bonds [66]. Consequently, the O—H bond in the Ib molecule ($n=5$) is comparatively weaker. Both the direct and indirect effects indicate that the absence of a conjugated system is a crucial characteristic for curcumin analogs as radical scavengers.

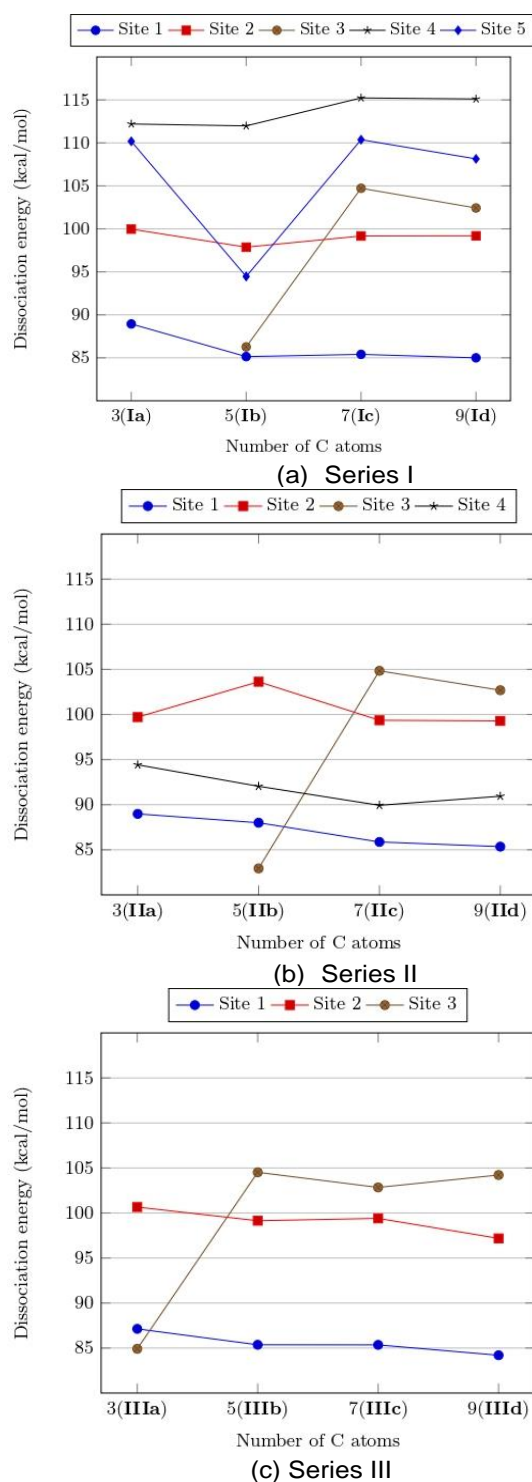


Figure 4. The calculated C–H and O–H bond dissociation energies against the number of carbon atoms (n) in the linker of the three series. The site numbering refers to Figure 1. The label inside the bracket in the x axis is the name code listed in Table 1.

The Gibbs Free Energies of HAT

The trend of Gibbs free energy of HAT was in line with the trend of dissociation energy. Like the dissociation energy, lengthening the linker decreased the value of ΔrG° of site 1 in three series gradually. Whereas, shortening the carbon chain decreased the ΔrG° of site 3 significantly at a certain value of n .

The values of ΔrG° at the two sites were less than zero. This means that the HAT occurring through sites 1 and 3 was thermodynamically favorable.

Table 2. The calculated Gibbs free energies of HAT at every value of n

n	The Gibbs free energy of reaction				
	Site 1	Site 2	Site 3	Site 4	Site 5
Series I					
3	2.70	13.26	n/a	25.01	21.34
5	-1.41	12.20	-2.46	24.25	3.70
7	-1.44	11.04	17.39	28.59	22.25
9	-2.45	11.96	16.00	28.20	19.10
Series II					
3	2.71	13.24	n/a	7.01	n/a
5	-0.23	14.21	-6.35	3.55	n/a
7	-1.32	12.43	16.41	4.23	n/a
9	-1.52	13.22	16.75	4.89	n/a
Series III					
3	-0.65	11.66	-4.60	n/a	n/a
5	-1.49	12.51	16.59	n/a	n/a
7	-3.08	12.44	15.37	n/a	n/a
9	-1.20	11.08	17.34	n/a	n/a

n/a means the data is not available.

The linker length affected the factors determining the Gibbs free energy of HAT at sites 1 and 3. Linker elongation reduced the enthalpy and entropy of the reactions at site 1 of the three series, as shown in Table S8. Conversely, linker shortening decreased the enthalpy but increased the entropy of the reactions at site 3 of certain molecules. Thus, enthalpy is the key factor determining $\Delta rG^\circ < 0$ at the phenolic O—H (Site 1 in Table 2), while enthalpy and entropy are the factors influencing $\Delta rG^\circ < 0$ at the C—H bond in the linker (Site 3 in Table 2) of Ib($n=5$), IIb($n=5$), and IIIa($n=3$). The increased entropy at site 3 of those molecules suggests that the absence of conjugated systems enhances system disorder.

The conjugated systems in the carbon linker impacted on free radical scavenging activity of curcumin. Somparn *et al.* [18] observed and found that curcumin analogs without a conjugated system on the seven carbon linker exhibited stronger scavenging activity compared to curcumin. Our findings, focusing on linker with fewer carbon atoms [Ib($n=5$), IIb($n=5$), and IIIa($n=3$)], align with their results, indicating that the absence of conjugated systems in the linker enhances the scavenging activity. Therefore, both studies highlight the significance of the absence of conjugated systems in enhancing curcumin's free radical scavenging activity.

Conclusions

In water solvents, both elongating and shortening curcumin linker length improves its $\cdot\text{OOH}$ scavenging activity thermodynamically. As the linker elongates, the $\cdot\text{OOH}$ scavenging activity through phenolic O—H improves gradually. On the other hand, as the linker shortens, the $\cdot\text{OOH}$ scavenging activity through the C—H bond in the linker improves significantly. The significant improvement was due to the absence of a conjugated system in the linker. Therefore, an analog without a conjugated system in the linker is most suitable as a radical scavenger.

The improvement in $\cdot\text{OOH}$ scavenging activity emphasizes the importance of considering the length of the curcumin linker without a conjugated system. Further exploration of scavenging reactions in different solvents expands the applicability of curcumin. Further development of curcumin analogs may offer promising opportunities for the design of efficient radical scavengers. These opportunities strengthen the potential of curcumin for applications in medicinal chemistry and beyond.

Conflicts of Interest

The authors declare that there is no conflict of interest regarding the publication of this paper.

Acknowledgment

This work was supported by Direktorat Riset, Teknologi, dan Pengabdian kepada Masyarakat Kementerian Pendidikan, Kebudayaan, Riset, dan Teknologi through “Penelitian Dasar Unggulan Perguruan Tinggi” (grant number 769/UN3.15/PT/2022). The authors thank Rizka Nur Fadilla (Osaka University, Japan) for the valuable discussions. LSPB gratefully acknowledges the Indonesia Endowment Fund for Education, the Ministry of Finance of Indonesia, for doctoral scholarship support and the 2019 Sandwich Program by the World Class University, Institut Teknologi Bandung for two months exchange to Kyushu University, Japan. All calculations are performed at the Research Institute for Information Technology, Kyushu University, Japan and in the “Riven” computer cluster at the Research Center for Quantum Engineering Design, Department of Physics, Faculty of Science and Technology, Universitas Airlangga, Indonesia. The authors contributions are as follows. L.S.P.B.: formal analysis, investigation, methodology, validation, writing—original draft and writing—review & editing; F.R.: conceptualization, methodology, writing—review & editing, and supervision; V.K.: formal analysis and validation; A.G.S.: formal analysis and validation; M.H.M.: writing—review & editing; K.Y.: writing—review & editing; H.R.: validation and supervision; H.K.D.: writing—review & editing and supervision.

References

- [1] S.C. Sharma, H. Mukhtar, S. K. Sharma, C. R. Krishna Murt. (1972). Lipid peroxide formation in experimental inflammation. *Biochemical Pharmacology*, 21(8), 1210-121421.
- [2] H. Yin, L. Xu, N. A. Porter. (2011). Free radical lipid peroxidation: Mechanisms and analysis. *Chem. Rev.* 111(10), 5944–5972.
- [3] D. Hahnel, K. Beyer, B. Engelmann, *Free Radical Biol. Med.* 27.9 (1999) 1087–1094.
- [4] U. Singh, A. Barik, B. G. Singh, K. I. Priyadarsini, *Free Rad. Res.* 45.3 (2011) 317–325.
- [5] A. Kunwar, A. Barik, S. K. Sandur, K. I. Priyadarsini, *Free Rad. Res.* 45.8 (2011) 959–965.
- [6] A. Banerjee, A. Kunwar, B. Mishra, and K.I. Priyadarsini, *Chem.-Biol. Interact.* 174.2 (2008) 134–139.
- [7] K.I. Priyadarsini, *Free Rad. Biol. Med.* 23.6 (1997) 838–843.
- [8] B. Cemil, K. Topuz, M. N. Demircan, G. Kurt, K. Tun, M. Kutlay, O. Ipcioglu, Z. Kucukodaci, *Acta Neurochir.* 152 (2010) 1583–1590.
- [9] R. Sanivarapu, V. Vallabhaneni, V. Verma, *Neurol. Res. Int.* (2016) 9468193.
- [10] R. Manikandan, R. Thiagarajan, S. Beulaja, G. Sudhandiran, M. Arumugam, *Free Radic. Biol. Med.* 48.4 (2010) 483–492.
- [11] A. S Darvesh, R. T Carroll, A. Bishayee, N. A Novotny, W. J Geldenhuys, C. J Van der Schyf. *Expert Opin. Investig. Drugs* 21.8 (2012) 1123–1140.
- [12] A. Monroy, G. J. Lithgow, S. Alavez, *Biofactors* 39.1 (2013) 122–132.
- [13] W. Park, A.R.M. R. Amin, Z. G. Chen, D. M. Shin, *Cancer Prev. Res. (Phila).* 6.5 (2013) 387–400.
- [14] A. Giordano, G. Tommonaro, *Nutrients* 11.10 (2019) 2376.
- [15] V. Calabrese, T. E. Bates, C. Mancuso, C. Cornelius, B. Ventimiglia, M. T. Cambria, L. Di Renzo, A. De Lorenzo, A. T. Dinkova-Kostova, *Mol. Nutr. Food Res.* 52.9 (2008) 1062–1073.
- [16] M. Bo, L. Jun, C. Hong, *Curr. Pharm. Des.* 19.11 (2013) 2101–2113.
- [17] L. Arshad, Md. A.I Haque, S.d N. A. Bukhari, I. Jantan, *Future Med. Chem.* 9.6 (2017) 605–626.
- [18] P. Somparn, C. Phisalaphong, S. Nakornchai, S. Unchern, N. P. Morales, *Biol. Pharm. Bull.* 30.1 (2007) 74–78.
- [19] W. M Weber, L. A Hunsaker, S. F Abcouwer, L. M Deck, D. L Vander Jagt, *Bioorg. Med. Chem.* 13.11 (2005) 3811–3820.
- [20] E. Ferrari, F. Pignedoli, C. Imbriano, G. Marverti, V. Basile, E. Venturi, M. Saladini, *J. Med. Chem.* 54.23 (2011) 8066–8077.
- [21] Q-T Zheng, Z-H Yang, L-Y Yu, Y-Y Ren, Q-X Huang, Q. Liu, X-Y Ma, Z-K Chen, Z-B Wang, X Zheng, *J. Asian Nat. Prod. Res.* 19(5) (2017) 489–503.
- [22] M. I. de Heer, P. Mulder, H-G Korth, K. U. Ingold, J. Luszytk, *J. Am. Chem. Soc.* 122.10 (2000) 2355–2360.
- [23] W-F Chen, S-L Deng, B Zhou, L Yang, Z-L Liu, *Free Radic. Biol. Med.* 40.3 (2006) 526–535.
- [24] K. Bairwa, J. Grover, M. Kania, S. M. Jachak, *RSC Adv.* 4.27 (2014) 13946–13978.
- [25] S. A. Nouredin, R. M. El-Shishtawy, K. O. Al-Footy, *Eur. J. Med. Chem* (2019) 111631.
- [26] Y-J Shang, X-L Jin, X-L Shang, J-J Tang, G-Y Liu, F Dai, Y-P Qian, G-J Fan, Q Liu, B Zhou, *Food Chem.* 119(4) (2010) 1435–1442.
- [27] L. Ross C. Barclay, M R. Vinqvist, K Mukai, H Goto, Y Hashimoto, A Tokunaga, H Uno, *Org Let* 2.18 (2000) 2841–2843.
- [28] G. W. Burton, T. Doba, E. Gabe, L. Hughes, F. L. Lee, L. Prasad, K U. Ingold, *J Am Chem Soc.* 107.24 (1985) 7053–7065.
- [29] A Galano, R Alvarez-Diduk, M T Ramirez-Silva, G Alarcon-Angeles, A Rojas-Hernandez, *Chem. Phys.* 363.1-3 (2009) 13–23.
- [30] S. V. Jovanovic, S. Steenken, C. W. Boone, M. G. Simic, *J Am Chem Soc.* 121.41 (1999) 9677–9681.
- [31] Y Manolova, V Deneva, L Antonov, E Drakalska, D Mo- mekova, N Lambov, *Spectrochim. Acta A.* 132 (2014) 815–820.
- [32] S Mondal, S Ghosh, S. P. Moulik, *J Photochem* 158 (2016) 212–218.
- [33] Y-M Sun, H-Y Zhang, D-Z Chen, C-B Liu, *Org Let.* 4.17 (2002) 2909–2911.
- [34] Q. Li, J. Chen, S. Luo, J. Xu, Q. Huang, T. Liu, *Eur. J. Med. Chem.* 93 (2015) 461–469.

- [35] L. Bedard, M. J. Young, D. Hall, T. Paul, K. U. Ingold, *J. Am. Chem. Soc.* 123.50 (2001) 12439–12448.
- [36] J. Aikens and T.A. Dix, *Arch. Biochem. Biophys.* 305.2 (1993), pp. 516–525.
- [37] J. Tomasi, B. Mennucci, E. Canc' es, *J. Mol. Struct.Theochem* 464 (1999) 211–226.
- [38] D. L. Baulch, R. A. Cox, R. F. Hampson Jr., J. A. Kerr, J.Troe, and R. T. Watson, *J. Phys. Chem. Ref. Data* 13 (1984) 1259.
- [39] A. Sinha, M. C. Hsiao, F. F Crim, *J. Chem. Phys.* 94 (1991) 4928.
- [40] K. Hassanzadeh, K. Akhtari, H. Hassanzadeh, S. Amir Zarei, N. Fakhraei, K. Hassanzadeh, *Food Chem* 164 (2014) 251–258.
- [41] F. A. Carey and R. J. Sundberg, *Advanced Organic Chemistry (Part A: Structure and Mechanisms)* (5th ed.), New York: Springer, 2007, P. 1001.
- [42] J. S. Wright, E. R. Johnson, G. A. DiLabio, *J. Am. Chem. Soc* 123.6 (2001) 1173–1183.
- [43] O. V. Dorofeeva and O. N. Ryzhova, *J. Phys. Chem. A* 120.15 (2016) 2471–2479.
- [44] P. Hohenberg and W. Kohn, *Phys. Rev.* 136.3B (1964), B864.
- [45] W. Kohn and L. J. Sham, *Phys. Rev. A* 140.4A (1965), A1133.
- [46] M. J. Frisch *et al.* Gaussian¹⁶ Revision C.01. Gaussian Inc. Wallingford CT. 2016.
- [47] M. H. Mahyuddin, A. Staykov, A. G. Saputro, M. K. Agusta, H. K. Dipojono, K. Yoshizawa, *J. Phys. Chem. C* 124 (2020) 18112-18125.
- [48] M. H. Mahyuddin, A. G. Saputro, R. P. P. Sukanli, F. Fathurrahman, J. Rizkiana, A. Nuruddina, H. K. Dipojono, *Phys. Chem. Chem. Phys.* 24 (2022) 4196.
- [49] R. Kishida, A. G. Saputro, R. L. Arevalo, H. Kasai, *Int. J. Quantum Chem* 117.23 (2017) e25445.
- [50] R. Kishida, A. G. Saputro, and H. Kasai, *Biochim. Biophys. Acta* 1850.2 (2015) 281–286.
- [51] Y. Zhao and D. G. Truhlar, *Theor. Chem. Acc.* 120 (2008) 215–241.
- [52] V. Khoirunisa, F. Rusydi, L.S.P. Boli, I. Puspitasari, H. Rachmawati, H. K. Dipojono, *R. Soc. Open Sci.* 8.201127 (2021) 1–10.
- [53] L.S.P. Boli, F. Rusydi, V. Khoirunisa, I. Puspitasari, H. Rachmawati, H. K. Dipojono, *Theor. Chem. Acc.* 140.94 (2021) 1–9.
- [54] M. Spiegel, A. Gamian, Z. Sroka, *Mol.* 26.16 (2021) 5058.
- [55] F. Rusydi, R. Madinah, I. Puspitasari, M.L.W. Fui, A. Ahmad, A. Rusydi, *Biochem. Mol. Biol. Educ.* 49.2 (2021) 216–227.
- [56] E. D. Glendening, A. E. Reed, J. E. Carpenter, and F. Weinhold. "NBO Version 3.1".
- [57] E. D. Glendening, C.R. Landis, F. Weinhold, *Wires Comput. Mol. Sci.* 2.1 (2011) 1–42.
- [58] P. Sanphui, N. R. Goud, U. B. Rao Khandavilli, S. Bhanoth, A. Nangia, *Chem. Commun.* 47 (2011) 5013–5015.
- [59] R. Benassi, E. Ferrari, S. Lazzari, F. Spagnolo, M. Saladini, *J. Mol. Struct.* 892 (2008) 168–176.
- [60] T. Brinck, M. Haerberlein, M. Jonsson, *J. Am. Chem. Soc.* 119.18 (1997) 4239– 4244.
- [61] K.I. Priyadarsini, D.K. Maity, G.H. Naik, M. S. Kumar, M.K. Unnikrishnan, J.G. Satav, H. Mohan, *Free Radic. Biol. Med.* 35.5 (2003) 475–484.
- [62] A. Barzegar and A. A. Moosavi-Movahedi, *PLoS ONE* 6(10) (2011) e26012.
- [63] D.K. Thbayh and B. Fiser, *Polym. Degrad. Stab.* 201 (2022) 109979.
- [64] Y. Zhao and D.G. Truhlar, *J. Phys. Chem. A* 112.6 (2008) 1095–1099.
- [65] Y. Sugiyama, S. Kawakishi, T. Osawa, *Biochem. Pharmacol.* 52.4 (1996) 519–525.
- [66] E. Arunan *et al.*, *Pure Appl. Chem.* 83.8 (2011) 1637–1641.

Appendix

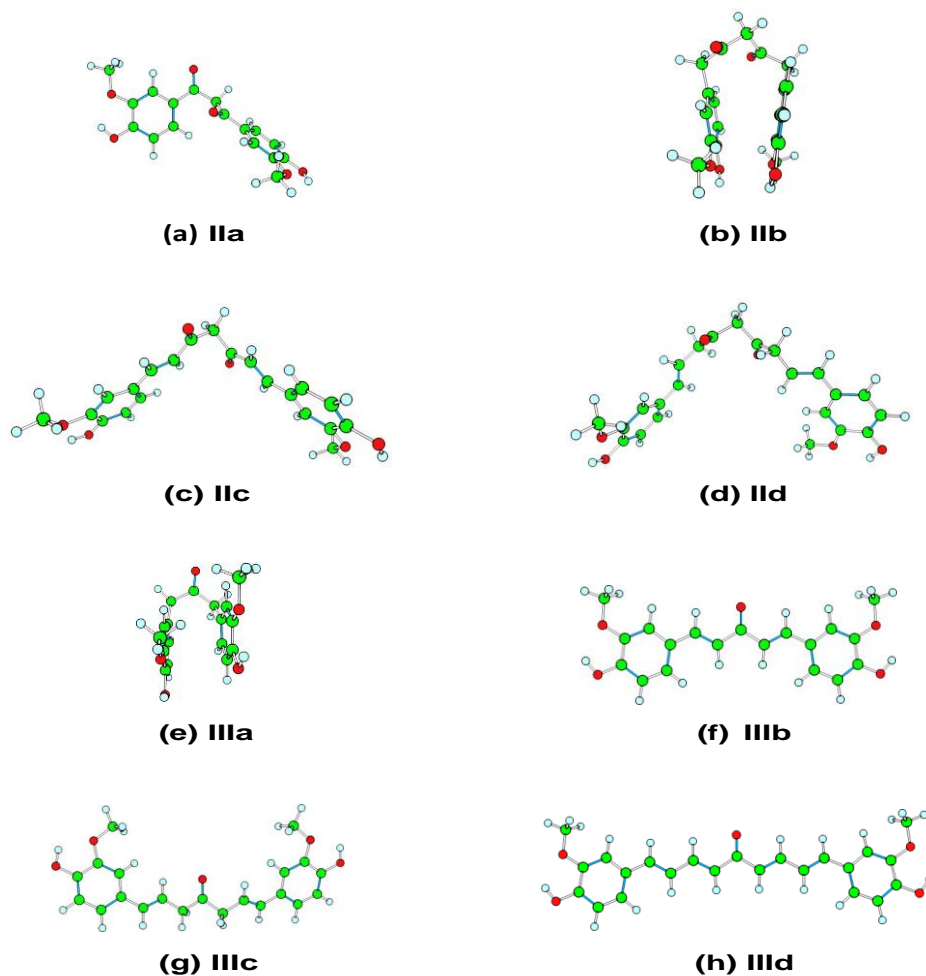


Figure S1. Optimized geometries of all members of series II (IIa - IIId) and III (IIIa - IIIId)

Table S1. Enthalpy of reaction (kcal/mol) (a) without and (b) with Polarizable Con-tinuum Model (PCM)

No.	Reaction	(a)	(b)
1.	$\text{H}^\bullet + \cdot\text{OOH} \rightarrow \text{HOOH}$	-77.32	-86.32
2.	$\text{H}^\bullet + \text{H}_2\text{O} \rightarrow \text{H}_2 + \text{OH}$	13.66	15.37

Table ESI-2. Cartesian coordinates of optimized geometries of the three series

No	X	Y	Z
1a			
8	-6.253143000	1.882516000	0.289073000
8	-6.135023000	-0.702796000	-0.175524000
8	-1.226849000	-1.877066000	-0.033570000
8	1.254891000	-1.876419000	-0.120345000

Continued on next page

No	X	Y	Z
8	6.105933000	-0.716973000	0.273743000
8	6.271847000	1.862076000	- 0.222207000
6	-6.129087000	- 2.106731000	- 0.402588000
6	-3.694215000	- 0.684822000	- 0.084381000
6	-4.935619000	- 0.084206000	- 0.022054000
6	- 5.036624000	1.299314000	0.224091000
6	- 3.891312000	2.056652000	0.402170000
6	- 2.640047000	1.451264000	0.331973000
6	- 2.530749000	0.083534000	0.088243000
6	-1.225533000	- 0.626075000	0.012272000
6	0.008135000	0.112374000	- 0.017737000
6	1.207018000	-0.554198000	- 0.093287000
6	2.524194000	0.104861000	- 0.135404000
6	2.658611000	1.467656000	- 0.397936000
6	3.916823000	2.057626000	- 0.427504000
6	5.047335000	1.291338000	- 0.194137000
6	4.921437000	- 0.085610000	0.066291000
6	3.671105000	- 0.674588000	0.090198000
6	6.076198000	- 2.119504000	0.508005000
1	- 6.927242000	1.203751000	0.145297000
1	-7.171345000	- 2.403132000	- 0.483574000
1	-5.659147000	- 2.628482000	0.434536000
1	-5.603181000	- 2.343172000	- 1.330565000
1	-3.591038000	- 1.745809000	- 0.267693000
1	- 3.991108000	3.117141000	0.597723000
1	- 1.762619000	2.064275000	0.486614000
1	0.296480000	-2.184336000	- 0.084690000
1	0.003977000	1.187688000	0.020670000
1	3.559558000	- 1.731628000	0.287490000
1	5.632083000	-2.640994000	- 0.343322000
1	5.514665000	- 2.345858000	1.417436000
1	7.111505000	- 2.426377000	0.628948000
1	1.791361000	2.080989000	- 0.604227000
1	4.035719000	3.113133000	- 0.638657000
1	6.933059000	1.178807000	- 0.044615000
Ib			
8	2.241547000	2.536577000	- 1.271791000
8	2.043788000	1.428270000	1.157515000
8	- 4.457143000	0.046409000	0.854727000
8	-3.815955000	- 2.285091000	- 0.131837000
8	2.862707000	- 1.717421000	0.945306000
8	3.409477000	-0.095721000	- 1.057156000
6	1.953386000	0.808155000	2.431818000
6	- 0.372012000	1.767599000	1.178986000
6	0.885091000	1.871163000	0.600200000
6	1.021369000	2.448027000	- 0.677185000
6	-0.095950000	2.945537000	- 1.323434000
6	-1.360667000	2.820159000	- 0.744253000
6	- 1.511573000	2.209534000	0.493174000
6	- 2.876425000	1.831694000	1.006904000
6	- 3.298413000	0.413790000	0.619513000
6	-2.325961000	- 0.459214000	0.008662000
6	-2.619708000	- 1.744455000	- 0.324279000
6	-1.622695000	- 2.684901000	- 0.950550000
6	-0.237198000	- 2.094263000	- 1.042116000

Continued on next page

No	X	Y	Z
6	0.113591000	-1.275093000	-2.108450000
6	1.337701000	-0.604727000	-2.121611000
6	2.218844000	-0.765135000	-1.068881000
6	1.893650000	-1.619980000	-0.004304000
6	0.668055000	-2.271929000	0.012317000
6	2.652910000	-2.629268000	2.015179000
1	2.817418000	1.832398000	-0.932641000
1	2.960319000	0.487638000	2.686674000
1	1.291122000	-0.061434000	2.388942000
1	1.583942000	1.515353000	3.179172000
1	-0.492178000	1.291627000	2.144814000
1	0.030504000	3.397025000	-2.300675000
1	-2.234224000	3.164140000	-1.287144000
1	-3.649598000	2.506346000	0.630900000
1	-2.920384000	1.874616000	2.100259000
1	-4.384907000	-1.587272000	0.273878000
1	-1.332123000	-0.098846000	-0.186761000
1	-1.625264000	-3.605632000	-0.359396000
1	-2.004307000	-2.949278000	-1.942365000
1	0.399390000	-2.911835000	0.844422000
1	2.518851000	-3.643817000	1.632336000
1	1.781305000	-2.341210000	2.608743000
1	3.546501000	-2.581692000	2.632115000
1	-0.583848000	-1.129504000	-2.926093000
1	1.610158000	0.054901000	-2.937266000
1	3.867992000	-0.317870000	-0.234156000

ic	X	Y	Z
8	8.817435000	1.825301000	0.001448000
8	8.563412000	-0.797365000	-0.000026000
8	1.238893000	-1.824032000	-0.001039000
8	-1.282622000	-1.812493000	-0.001655000
8	-8.549635000	-0.805106000	0.001923000
8	-8.817790000	1.816796000	0.000066000
6	8.480736000	-2.216907000	-0.000755000
6	6.123342000	-0.633915000	-0.000142000
6	7.398909000	-0.096451000	0.000262000
6	7.570989000	1.298378000	0.001045000
6	6.462792000	2.132818000	0.001403000
6	5.183579000	1.591794000	0.000987000
6	4.995210000	0.206748000	0.000212000
6	3.673684000	-0.417178000	-0.000261000
6	2.482598000	0.201132000	-0.000147000
6	1.229199000	-0.572123000	-0.000703000
6	-0.006065000	0.167048000	-0.000389000
6	-1.214152000	-0.487291000	-0.000822000
6	-2.477708000	0.231408000	-0.000481000
6	-3.662063000	-0.402647000	-0.000929000
6	-4.986263000	0.216760000	-0.000767000
6	-5.182037000	1.600763000	-0.001765000
6	-6.464205000	2.135284000	-0.001484000
6	-7.568359000	1.295906000	-0.000203000
6	-7.388914000	-0.097856000	0.000745000
6	-6.110612000	-0.629015000	0.000420000
6	-8.459544000	-2.224164000	0.002464000
1	9.456450000	1.099420000	0.001121000

No	X	Y	Z
1	9.505331000	-2.578316000	-0.000843000
1	7.963540000	-2.571227000	-0.895475000
1	7.963373000	-2.572133000	0.893509000
1	5.981569000	-1.707491000	-0.000743000
1	6.618766000	3.204718000	0.002011000
1	4.332560000	2.261158000	0.001280000
1	3.660702000	-1.504977000	-0.000777000
1	2.389611000	1.281158000	0.000335000
1	-0.335246000	-2.134984000	-0.001912000
1	0.010366000	1.247478000	0.000189000
1	-2.400576000	1.312267000	0.000186000
1	-3.649720000	-1.489422000	-0.001376000
1	-5.964150000	-1.701955000	0.001131000
1	-7.939993000	-2.575928000	0.896833000
1	-7.940887000	-2.576659000	-0.892136000
1	-9.482245000	-2.590925000	0.003132000
1	-4.335616000	2.275885000	-0.002889000
1	-6.625042000	3.206479000	-0.002309000
1	-9.453045000	1.087688000	0.000849000
Id			
8	9.585680000	1.879752000	-0.084100000
8	7.497414000	4.428255000	-0.012599000
8	1.192289000	3.245190000	0.757109000
8	-1.114356000	3.372552000	-1.025424000
8	-7.534439000	1.295882000	-0.305215000
8	-8.974169000	-1.627695000	-0.328247000
6	6.410322000	-2.628269000	-0.490598000
6	5.943325000	-2.469893000	-0.524638000
6	7.209238000	0.312944000	-0.621307000
6	8.347713000	-0.265945000	2.040039000
6	8.195637000	-2.671076000	-0.400748000
6	6.917318000	-0.566201000	1.673843000
6	5.781097000	-2.484340000	-0.644834000
6	4.456766000	0.742601000	1.124684000
6	3.274195000	3.032731000	1.295520000
6	0.962797000	2.091197000	2.400273000
6	-0.279086000	3.727798000	1.887095000
6	-1.245168000	-2.081220000	-2.004360000
6	-3.702272000	-0.725055000	-2.707227000
6	-4.538985000	2.254242000	-0.988347000
6	-5.687496000	-2.349763000	1.317353000
6	-6.479042000	-1.511179000	-0.739776000
6	-7.582194000	-1.301895000	-1.704958000
6	-7.902990000	-2.593583000	-0.710492000
6	-7.111430000	-2.742868000	2.334988000
6	-6.018375000	-3.189395000	0.622514000
6	-6.802389000	1.879752000	-0.084100000
1	9.486526000	4.428255000	-0.012599000
1	6.850677000	3.245190000	0.757109000
1	5.761831000	3.372552000	-1.025424000
1	5.832175000	1.295882000	-0.305215000
1	5.076707000	-1.627695000	-0.328247000
1	9.079200000	-2.628269000	-0.490598000
1	6.807148000	-2.469893000	-0.524638000
1	4.475721000	0.312944000	-0.621307000

Continued on next page

No	X	Y	Z
1	3.204879000	- 0.265945000	2.040039000
1	-0.228756000	- 2.671076000	- 0.400748000
1	-0.440927000	- 0.566201000	1.673843000
1	-3.810786000	- 2.484340000	- 0.644834000
1	- 4.383828000	0.742601000	1.124684000
1	- 5.417138000	3.032731000	1.295520000
1	- 5.770658000	2.091197000	2.400273000
1	- 6.815499000	3.727798000	1.887095000
1	-7.301746000	- 2.081220000	- 2.004360000
1	-6.234910000	- 0.725055000	- 2.707227000
1	-8.198606000	2.254242000	- 0.988347000
1	-9.033871000	- 2.349763000	1.317353000
6	-2.558542000	- 1.511179000	- 0.739776000
6	1.979590000	-1.301895000	- 1.704958000
1	1.499231000	-2.593583000	- 0.710492000
1	2.136514000	- 2.742868000	2.334988000
1	-2.664831000	- 3.189395000	0.622514000
1	-2.548573000	1.879752000	- 0.084100000
IIa			
8	-6.176381000	0.066911000	- 1.224634000
8	- 5.259441000	1.401039000	0.843256000
8	-0.479976000	- 0.289103000	1.469373000
8	1.830997000	- 2.665136000	0.915886000
8	5.749715000	0.556676000	0.301321000
8	4.780010000	2.523679000	- 1.146298000
6	- 4.816062000	2.145494000	1.971528000
6	- 3.084436000	0.302987000	0.685098000
6	- 4.381291000	0.535027000	0.276651000
6	-4.906874000	- 0.163639000	- 0.831216000
6	-4.124073000	- 1.081026000	- 1.511384000
6	-2.813671000	- 1.310518000	- 1.101738000
6	-2.288752000	- 0.624997000	- 0.009031000
6	-0.901416000	- 0.844084000	0.474523000
6	-0.012233000	- 1.808728000	- 0.302209000
6	1.415726000	- 1.768364000	0.209721000
6	2.278132000	-0.620024000	- 0.173325000
6	1.804511000	0.443380000	- 0.937705000
6	2.644223000	1.504247000	- 1.264846000
6	3.958663000	1.500472000	- 0.829669000
6	4.445632000	0.427548000	- 0.053895000
6	3.610492000	- 0.621121000	0.272632000
6	6.324099000	- 0.480088000	1.087665000
1	-6.565780000	0.729875000	- 0.637264000
1	- 5.654346000	2.769230000	2.268861000
1	- 3.962705000	2.773202000	1.704988000
1	- 4.544019000	1.474890000	2.789793000
1	- 2.657905000	0.822166000	1.533118000
1	-4.549720000	- 1.607020000	- 2.356694000
1	-2.218841000	- 2.034724000	- 1.643313000
1	-0.053737000	- 1.589020000	- 1.370779000
1	-0.394411000	- 2.821913000	- 0.155306000
1	3.957815000	- 1.455184000	0.868018000
1	6.288755000	- 1.431636000	0.552210000
1	5.801330000	- 0.570810000	2.042563000
1	7.357312000	- 0.191173000	1.258711000

Continued on next page

No	X	Y	Z
1	0.779258000	0.469514000	- 1.285885000
1	2.291443000	2.339481000	- 1.856803000
1	5.650156000	2.351192000	- 0.760248000
IIb			
8	2.610128000	2.063028000	1.268696000
8	2.527203000	1.036933000	- 1.167341000
8	-3.179412000	- 0.453898000	- 1.901848000
8	-2.611764000	- 0.189539000	2.369174000
8	2.428843000	- 0.927961000	1.398637000
8	2.999990000	-1.896297000	- 0.999125000
6	2.571393000	0.700096000	- 2.548916000
6	0.109142000	1.360040000	- 1.304971000
6	1.331192000	1.436679000	- 0.656259000
6	1.406165000	1.960305000	0.645652000
6	0.255028000	2.391203000	1.280093000
6	- 0.972615000	2.325638000	0.619291000
6	-1.054427000	1.817212000	- 0.671607000
6	-2.374399000	1.742502000	- 1.412962000
6	-3.085156000	0.441161000	- 1.095162000
6	- 3.676538000	0.303655000	0.302943000
6	-2.856382000	- 0.565519000	1.246807000
6	-2.395316000	- 1.920038000	0.747528000
6	-0.961038000	- 1.857382000	0.251825000
6	-0.628726000	- 2.308526000	- 1.018444000
6	0.701613000	-2.318298000	- 1.442417000
6	1.700316000	-1.867748000	- 0.598728000
6	1.367320000	- 1.383389000	0.677634000
6	0.048474000	- 1.384675000	1.100850000
6	2.195972000	- 0.581460000	2.758709000
1	3.262780000	1.586266000	0.738003000
1	3.610639000	0.472958000	- 2.770817000
1	2.233948000	1.545108000	- 3.154375000
1	1.955784000	-0.178389000	- 2.753193000
1	0.046956000	0.957359000	- 2.308767000
1	0.330867000	2.797306000	2.282110000
1	- 1.862272000	2.694222000	1.117425000
1	-2.214025000	1.783133000	- 2.490235000
1	-4.642062000	- 0.199640000	0.185965000
1	- 3.828768000	1.271962000	0.776238000
1	-2.465928000	- 2.611482000	1.590780000
1	-0.212375000	- 1.018896000	2.086279000
1	1.809719000	- 1.443632000	3.308210000
1	1.496328000	0.254133000	2.830952000
1	3.159468000	- 0.282718000	3.163116000
1	-1.407284000	- 2.658279000	- 1.686135000
1	0.973169000	-2.680376000	- 2.427427000
1	3.521853000	-1.402357000	- 0.352468000
1	-3.016986000	2.575179000	- 1.116638000
1	-3.043812000	- 2.268710000	- 0.055761000
IIc			
8	6.721623000	- 2.126531000	1.706037000
8	6.447530000	-2.112147000	- 0.913260000
8	0.881311000	2.685055000	- 2.012866000
8	- 0.881319000	2.684627000	2.013397000
8	-6.447329000	- 2.112545000	0.912839000

Continued on next page

No	X	Y	Z
8	-6.721792000	- 2.126027000	- 1.706444000
6	6.342232000	-2.138882000	- 2.331168000
6	4.620445000	-0.492051000	- 0.785505000
6	5.595366000	-1.302841000	- 0.231532000
6	5.769185000	- 1.335349000	1.163244000
6	4.964006000	- 0.555821000	1.981462000
6	3.986302000	0.257119000	1.424075000
6	3.801016000	0.300807000	0.039129000
6	2.789389000	1.136633000	- 0.599543000
6	1.912490000	1.958352000	0.000058000
6	0.950191000	2.740451000	- 0.799960000
6	- 0.000004000	3.622911000	0.000364000
6	- 0.950215000	2.740297000	0.800506000
6	- 1.912493000	1.958342000	0.000327000
6	- 2.789481000	1.136601000	0.599770000
6	-3.801147000	0.300945000	- 0.039065000
6	-3.986625000	0.257741000	- 1.424001000
6	-4.964350000	- 0.555066000	- 1.981545000
6	-5.769347000	- 1.334961000	- 1.163497000
6	-5.595332000	- 1.302938000	0.231267000
6	-4.620409000	- 0.492263000	0.785397000
6	-6.341525000	- 2.140032000	2.330694000
1	7.180213000	- 2.589357000	0.991224000
1	7.099932000	-2.836874000	- 2.676227000
1	6.534217000	-1.147977000	- 2.749186000
1	5.352555000	-2.486669000	- 2.636348000
1	4.478920000	-0.459866000	- 1.858665000
1	5.116328000	- 0.597215000	3.053024000
1	3.368728000	0.858273000	2.079412000
1	2.746520000	1.084743000	- 1.685725000
1	1.873425000	2.083829000	1.076598000
1	-0.564005000	4.242712000	- 0.697805000
1	0.564002000	4.242555000	0.698668000
1	-1.873360000	2.083961000	- 1.076194000
1	- 2.746646000	1.084532000	1.685945000
1	-4.478751000	- 0.460449000	1.858552000
1	-6.533505000	- 1.149382000	2.749319000
1	-5.351686000	- 2.487834000	2.635327000
1	-7.099001000	- 2.838322000	2.675644000
1	-3.369208000	0.859197000	- 2.079208000
1	-5.116826000	- 0.596078000	- 3.053100000
1	-7.180195000	- 2.589202000	- 0.991738000
IIa			
8	8.195083000	- 2.444385000	0.257393000
8	5.698904000	-3.123799000	- 0.229287000
8	1.290412000	2.218190000	- 1.718772000
8	- 1.447147000	2.889334000	1.068050000
8	-7.295177000	- 0.970172000	1.511859000
8	-7.422512000	- 3.234280000	0.173901000
6	4.370790000	-3.553028000	- 0.494204000
6	4.910128000	- 0.842567000	0.148372000
6	5.893440000	- 1.812065000	0.076675000
6	7.239241000	- 1.483047000	0.330141000
6	7.576454000	- 0.181568000	0.648525000
6	6.582760000	0.795112000	0.719173000

Continued on next page

No	X	Y	Z
6	5.246456000	0.484324000	0.475350000
6	2.917358000	1.430013000	0.429750000
6	1.967676000	2.577951000	0.557018000
6	1.135975000	2.821947000	-0.684354000
6	0.022415000	3.855175000	-0.539725000
6	-1.224464000	3.093066000	-0.101330000
6	-2.112233000	2.589923000	-1.219518000
6	-3.217732000	1.696162000	-0.754757000
6	-4.454840000	-0.489984000	-0.816665000
6	-4.558949000	-1.705288000	-1.490303000
6	-5.552260000	-2.629177000	-1.164552000
6	-6.451640000	-2.344158000	-0.155155000
6	-6.355483000	-1.122703000	0.539232000
6	-5.370728000	-0.208036000	0.213930000
6	-7.279389000	0.234032000	2.265457000
1	7.768527000	-3.280330000	0.025268000
1	4.433700000	-4.616604000	-0.707771000
1	3.960728000	-3.026904000	-1.359690000
1	3.731494000	-3.388544000	0.376573000
1	3.880670000	-1.108186000	-0.051565000
1	8.615269000	0.059056000	0.840061000
1	6.855747000	1.813710000	0.970746000
1	2.467632000	0.464575000	0.215301000
1	2.491694000	3.511721000	0.788019000
1	-0.136479000	4.333381000	-1.505653000
1	0.271508000	4.587149000	0.227763000
1	-2.508254000	3.487803000	-1.712922000
1	-3.890483000	2.120567000	-0.015264000
1	-5.303212000	0.723102000	0.760541000
1	-7.432478000	1.098223000	1.614496000
1	-6.334871000	0.339309000	2.804732000
1	-8.099762000	0.158256000	2.973980000
1	-3.857536000	-1.936877000	-2.283846000
1	-5.635014000	-3.573343000	-1.689387000
1	-7.945560000	-2.860870000	0.896078000
6	4.238534000	1.553603000	0.570003000
6	-3.393147000	0.453130000	-1.206907000
1	4.642991000	2.540885000	0.786298000
1	1.254297000	2.424995000	1.378219000
1	-2.697973000	0.072800000	-1.953414000
1	-1.471314000	2.100111000	-1.960657000
IIIa			
8	2.534148000	-2.142261000	-1.110100000
8	3.356692000	-0.045026000	0.265258000
8	-0.236896000	3.717453000	0.852263000
8	-0.208353000	-2.275011000	1.395578000
8	-1.938888000	-3.266816000	-0.322913000
6	3.793940000	1.026266000	1.090423000
6	1.465119000	1.303900000	-0.502125000
6	2.216232000	0.139913000	-0.458064000
6	1.808133000	-0.993134000	-1.181881000
6	0.667178000	-0.934056000	-1.959951000
6	-0.089881000	0.237446000	-1.999317000
6	0.290539000	1.352058000	-1.264996000
6	-0.583367000	2.593542000	-1.217570000

Continued on next page

No	X	Y	Z
6	- 0.920465000	2.937870000	0.225728000
6	- 2.126729000	2.261595000	0.863314000
6	- 2.156225000	0.772715000	0.610357000
6	-3.063031000	0.206504000	- 0.273278000
6	-3.005070000	- 1.156219000	- 0.578232000
6	-2.029466000	- 1.947401000	- 0.005364000
6	-1.116754000	- 1.386651000	0.907461000
6	-1.188788000	- 0.041127000	1.220179000
6	0.790931000	- 1.780710000	2.276286000
1	3.280467000	-1.991505000	- 0.514963000
1	4.690093000	0.673806000	1.593948000
1	3.028998000	1.279754000	1.829482000
1	4.030894000	1.906189000	0.487778000
1	1.762668000	2.171417000	0.074555000
1	0.363090000	-1.816378000	- 2.511275000
1	-1.005734000	0.260376000	- 2.578166000
1	-1.500171000	2.410887000	- 1.781982000
1	- 3.017132000	2.726685000	0.427108000
1	- 0.473681000	0.402218000	1.903893000
1	0.338266000	- 1.377506000	3.185579000
1	1.387666000	- 1.008367000	1.783935000
1	1.421626000	- 2.630156000	2.525419000
1	-3.814357000	0.827920000	- 0.747908000
1	-3.702145000	- 1.606135000	- 1.275189000
1	-1.186226000	- 3.639999000	0.154978000
1	-0.063040000	3.453356000	- 1.644973000
1	- 2.108673000	2.495653000	1.929280000
IIIb			
8	7.581988000	- 1.736600000	0.000231000
8	7.338140000	0.886728000	0.000396000
8	0.000000000	1.928963000	- 0.000340000
8	- 7.338140000	0.886728000	0.000228000
8	-7.581988000	- 1.736600000	- 0.000083000
6	7.261033000	2.306579000	0.000473000
6	4.897421000	0.732585000	0.000115000
6	6.170931000	0.190400000	0.000220000
6	6.337720000	- 1.205108000	0.000137000
6	5.226409000	-2.035621000	- 0.000054000
6	3.949298000	-1.489873000	- 0.000151000
6	3.766226000	-0.104032000	- 0.000059000
6	2.447236000	0.524769000	- 0.000141000
6	1.252005000	-0.085715000	- 0.000071000
6	0.000000000	0.703816000	- 0.000186000
6	-1.252005000	- 0.085715000	- 0.000129000
6	-2.447236000	0.524769000	- 0.000238000
6	-3.766226000	- 0.104032000	- 0.000217000
6	-3.949298000	- 1.489873000	- 0.000385000
6	-5.226409000	- 2.035621000	- 0.000340000
6	-6.337720000	- 1.205108000	- 0.000126000
6	- 6.170931000	0.190400000	0.000034000
6	-4.897421000	0.732585000	- 0.000021000
6	- 7.261033000	2.306579000	0.000349000
1	8.223761000	- 1.013091000	0.000346000
1	8.287044000	2.663940000	0.000611000
1	6.745064000	2.663323000	0.894932000

Continued on next page

No	X	Y	Z
1	6.745267000	2.663430000	- 0.894061000
1	4.759612000	1.806667000	0.000174000
1	5.378449000	-3.108077000	- 0.000132000
1	3.095549000	-2.155736000	- 0.000317000
1	2.439544000	1.612920000	- 0.000258000
1	1.156132000	- 1.165607000	0.000075000
1	-1.156132000	- 1.165607000	0.000011000
1	-2.439544000	1.612920000	- 0.000338000
1	- 4.759612000	1.806667000	0.000095000
1	-6.745247000	2.663457000	- 0.894162000
1	- 6.745083000	2.663296000	0.894831000
1	- 8.287044000	2.663940000	0.000476000
1	-3.095549000	- 2.155736000	- 0.000574000
1	-5.378449000	- 3.108077000	- 0.000480000
1	-8.223761000	- 1.013091000	0.000054000
IIIc			
8	- 8.500475000	1.143692000	0.495717000
8	-6.599815000	2.074504000	- 1.070658000
8	0.000151000	- 0.124753000	0.000366000
8	6.599246000	2.074830000	1.070777000
8	8.500755000	1.143601000	- 0.494317000
6	-5.614481000	2.623825000	- 1.934754000
6	-5.053504000	0.308195000	- 0.393921000
6	-6.271145000	0.962820000	- 0.358320000
6	- 7.309201000	0.492136000	0.469098000
6	-7.105898000	- 0.628671000	1.250489000
6	-5.876262000	- 1.286736000	1.212990000
6	-4.840658000	- 0.836095000	0.396815000
6	-3.565736000	- 1.573247000	0.392083000
6	-2.497814000	- 1.331064000	- 0.370479000
6	-1.245265000	- 2.146987000	- 0.310504000
6	0.000109000	-1.333975000	- 0.000162000
6	1.245434000	- 2.147340000	0.309466000
6	2.498050000	- 1.331562000	0.370043000
6	3.565788000	-1.573005000	- 0.393011000
6	4.840737000	-0.835895000	- 0.397225000
6	5.876755000	-1.286705000	- 1.212783000
6	7.106467000	-0.628749000	- 1.249654000
6	7.309419000	0.492134000	- 0.468280000
6	6.270918000	0.963032000	0.358457000
6	5.053197000	0.308518000	0.393433000
6	5.613531000	2.624229000	1.934389000
1	-8.449497000	1.893681000	- 0.111935000
1	-6.072939000	3.490945000	- 2.402372000
1	-5.326966000	1.899636000	- 2.700769000
1	-4.733576000	2.932755000	- 1.367016000
1	-4.262605000	0.682540000	- 1.030049000
1	-7.911725000	- 0.979629000	1.883857000
1	-5.725368000	- 2.165901000	1.829124000
1	-3.520981000	- 2.406269000	1.091544000
1	-2.496617000	- 0.512167000	- 1.083768000
1	1.327460000	-2.957061000	- 0.421667000
1	1.050239000	- 2.631633000	1.276077000
1	2.497093000	- 0.513439000	1.084223000
1	3.520882000	-2.405360000	- 1.093256000

Continued on next page

No	X	Y	Z
1	4.261903000	0.683088000	1.028938000
1	5.325618000	1.900074000	2.700286000
1	4.732909000	2.933191000	1.366231000
1	6.071812000	3.491339000	2.402196000
1	5.726136000	-2.165934000	-1.828894000
1	7.912626000	-0.979846000	-1.882524000
1	8.449490000	1.893673000	0.113209000
1	-1.050070000	-2.630522000	-1.277497000
1	-1.327383000	-2.957297000	0.419968000
IIId			
8	10.083537000	-1.720641000	-0.000063000
8	9.780351000	0.898438000	-0.000030000
8	0.000000000	1.915349000	0.000065000
8	-9.780351000	0.898438000	0.000075000
8	-10.083537000	-1.720641000	-0.000010000
6	9.671836000	2.316004000	0.000003000
6	7.343548000	0.690686000	0.000011000
6	8.628748000	0.175631000	-0.000019000
6	8.826644000	-1.215329000	-0.000039000
6	7.733086000	-2.067918000	-0.000025000
6	6.443777000	-1.549793000	0.000002000
6	6.229101000	-0.168301000	0.000015000
6	4.895700000	0.432788000	0.000038000
6	3.714094000	-0.213148000	-0.000094000
6	2.457085000	0.497267000	-0.000039000
6	0.000000000	0.688460000	-0.000057000
6	-2.457085000	0.497267000	-0.000023000
6	-3.714094000	-0.213148000	-0.000067000
6	-4.895700000	0.432788000	0.000063000
6	-6.229101000	-0.168301000	0.000047000
6	-6.443777000	-1.549793000	0.000004000
6	-7.733086000	-2.067918000	-0.000014000
6	-8.826644000	-1.215329000	0.000009000
6	-8.628748000	0.175631000	0.000056000
6	-7.343548000	0.690686000	0.000078000
6	-9.671836000	2.316004000	0.000202000
1	10.708987000	-0.983231000	-0.000066000
1	10.689700000	2.696098000	-0.000006000
1	9.148229000	2.661599000	0.894432000
1	9.148200000	2.661638000	-0.894395000
1	7.184377000	1.761857000	0.000028000
1	7.906992000	-3.137144000	-0.000032000
1	5.606457000	-2.236083000	0.000024000
1	4.875332000	1.520955000	0.000169000
1	3.667787000	-1.298338000	-0.000244000
1	-2.493147000	1.584945000	0.000108000
1	-3.667787000	-1.298338000	-0.000210000
1	-4.875332000	1.520955000	0.000190000
1	-7.184377000	1.761857000	0.000115000
1	-9.148220000	2.661699000	-0.894184000
1	-9.148209000	2.661538000	0.894643000
1	-10.689700000	2.696098000	0.000241000
1	-5.606457000	-2.236083000	-0.000005000
1	-7.906992000	-3.137144000	-0.000042000
1	-10.708987000	-0.983231000	0.000040000

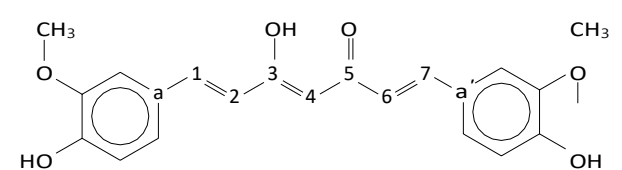
Continued on next page

No	X	Y	Z
1	2.493147000	1.584945000	0.000096000
6	-1.250288000	-0.098065000	-0.000127000
6	1.250288000	-0.098065000	-0.000138000
1	-1.168309000	-1.180389000	-0.000255000
1	1.168309000	-1.180389000	-0.000268000

Table S3. Geometrical parameters of **1c** and **11c** calculated using M06-2X (Calc.) compared to the literature values (Lite.) [1].

No.	Parameter	Calc.	Lite.
1c			
1.	O ³ – H ³	1.001	0.940
2.	C ³ – O ³	1.327	1.310
3.	C ⁵ = O ⁵	1.252	1.270
4.	C ³ = C ⁴	1.370	1.374
5.	C ⁴ – C ⁵	1.440	1.420
11c			
6.	C ³ – O ³	1.216	
7.	C ⁵ – O ⁵	1.216	
8.	C ³ – C ⁴	1.524	
9.	C ⁴ – C ⁵	1.524	

Table S4. The bonding orbital of C1-C2 bond in the carbon linker of the three series is shown as a linear combination of atomic orbital $aC1(sp^\alpha) + bC2(sp^\beta)$. $\alpha + \beta = 2.00$ indicates a C=C bond, while $\alpha + \beta \geq 3.00$ indicates a C-C bond. The Labels for the atoms in the "Parameter" section are based on the provided figure (**1c**)



No	Parameter	a	α	b	β
1a					
1	a-1	0.71	2.21	0.71	2.37
2	1-2	0.71	2.79	0.71	1.96
3	2-3,	0.70	1.97	0.71	2.89
4	3-a	0.71	2.34	0.71	2.19
1b					
5	a-1	0.71	2.21	0.71	2.37
6	1-2	0.71	2.79	0.71	1.96
7	2-3	0.70	1.44	0.71	1.82
8	3-4	0.72	2.04	0.70	1.72
9	4-5,	0.70	1.97	0.71	2.89
10	5-a	0.71	2.34	0.71	2.19
1c					
11	a-1	0.72	2.11	0.69	1.88
12	1-2	0.67	1.00	0.74	1.00
13	2-3	0.70	2.04	0.71	1.86
14	3-4	0.62	1.00	0.79	1.00
15	4-5	0.71	1.97	0.70	1.76
16	5-6	0.72	1.87	0.71	2.07
17	6-7,	0.74	1.00	0.67	1.00
18	7-a	0.69	1.88	0.72	2.10

Continued on next page

No	Parameter	a	α	b	β
Id					
19	a-1	0.72	2.09	0.70	1.96
20	1-2	0.71	1.00	0.71	1.00
21	2-3	0.72	2.52	0.70	2.11
22	3-4	0.71	2.72	0.71	1.95
23	4-5	0.71	1.43	0.71	1.76
24	5-6	0.71	2.03	0.70	1.73
25	6-7	0.70	1.92	0.71	2.80
26	7-8	0.72	2.36	0.70	2.07
27	8-9	0.71	1.00	0.71	1.00
28	9-a	0.70	1.95	0.72	2.09
Ila					
29	a-1	0.72	2.24	0.69	1.81
30	1-2	0.69	1.95	0.72	2.68
31	2-3	0.72	2.78	0.69	1.98
32	3-a	0.69	1.75	0.72	2.25
Ilb					
33	a-1	0.70	2.28	0.71	2.53
34	1-2	0.72	2.86	0.70	1.82
35	2-3	0.69	1.96	0.72	2.74
36	3-4	0.72	2.70	0.69	1.95
37	4-5	0.70	1.82	0.72	2.88
38	5-a	0.71	2.50	0.71	2.26
Ilc					
39	a-1	0.72	2.10	0.70	1.87
40	1-2	0.66	1.00	0.75	1.00
41	2-3	0.71	2.15	0.70	1.79
42	3-4	0.69	2.00	0.72	2.80
43	4-5	0.72	2.80	0.69	2.00
44	5-6	0.70	1.79	0.71	2.15
45	6-7	0.75	1.00	0.66	1.00
46	7-a	0.70	1.87	0.72	2.10
IId					
47	a-1	0.72	2.09	0.70	1.96
48	1-2	0.71	1.54	0.70	1.53
49	2-3	0.70	2.07	0.72	2.34
50	3-4	0.72	2.87	0.70	1.79
51	4-5	0.69	1.97	0.72	2.87
52	5-6	0.72	2.87	0.69	1.97
53	6-7	0.70	1.79	0.72	2.87
54	7-8	0.72	2.34	0.70	2.07
55	8-9	0.71	1.55	0.71	1.52
56	9-a	0.70	1.95	0.72	2.09
Ila					
57	a-1	0.71	2.23	0.71	2.41
58	1-2	0.72	2.87	0.70	1.87
59	2-3	0.70	1.88	0.72	2.86
60	3-a	0.71	2.52	0.71	2.26
Ilb					
61	a-1	0.72	2.09	0.70	1.86
62	1-2	0.67	1.00	0.74	1.00
63	2-3	0.71	2.10	0.70	1.87
64	3-4	0.70	1.88	0.71	2.13
65	4-5	0.75	1.00	0.67	1.00
66	5-a	0.69	1.88	0.72	2.11
Ilc					
67	a-1	0.72	2.09	0.70	1.95
68	1-2	0.71	1.00	0.71	1.00
69	2-3	0.70	2.07	0.72	2.35
70	3-4	0.72	2.84	0.69	1.87
71	4-5	0.69	1.87	0.72	2.84
72	5-6	0.72	2.35	0.70	2.07
73	6-7	0.71	1.00	0.71	1.00

Continued on next page

Table 4 – Continued from previous page

No	Parameter	a	α	b	β
74	7-a	0.70	1.95	0.72	2.09
III d					
75	a-1	0.71	2.07	0.70	1.91
76	1-2	0.69	1.00	0.72	1.00
77	2-3	0.71	1.96	0.71	1.90
78	3-4	0.74	1.00	0.67	1.00
79	4-5	0.71	2.10	0.71	1.88
80	5-6	0.70	1.87	0.71	2.07
81	6-7	0.75	1.00	0.67	1.00
82	7-8	0.70	1.93	0.71	1.95
83	8-9	0.72	1.00	0.69	1.00
84	9-a	0.70	1.90	0.71	2.08

Table S5. Charges of the radicalized oxygen atom (O) and a hydrogen atom (H) in the methoxy group of the radical forms of the three series.

Molecules	n	NBO charges (e)	
		O	H
Ia	3	-0.584	0.194
Ib	5	-0.630	0.194
Ic	7	-0.594	0.192
Id	9	-0.604	0.192
IIa	3	-0.580	0.195
IIb	5	-0.599	0.198
IIc	7	-0.589	0.193
IId	9	-0.604	0.190
IIIa	3	-0.597	0.192
IIIb	5	-0.593	0.192
IIIc	7	-0.604	0.192
IIId	9	-0.601	0.191

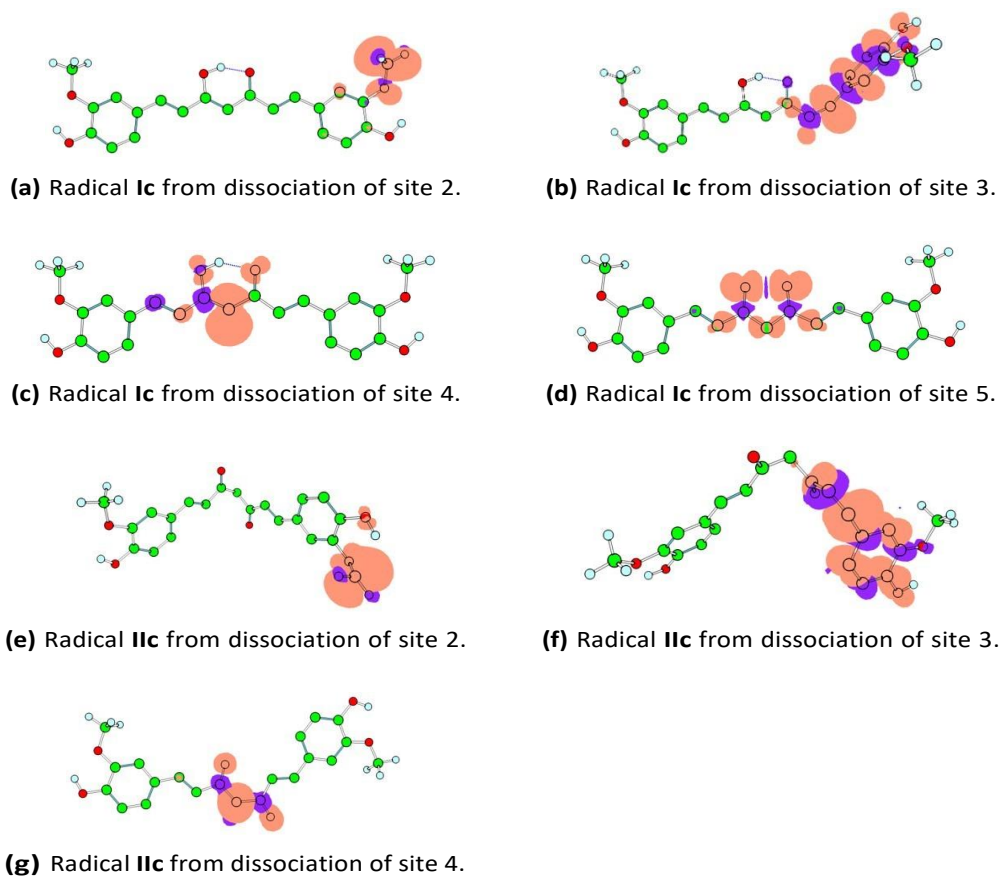


Figure S2. Spin density of the radical forms of **Ic** and **IIc** with an isosurface of 0.002. Some hydrogen atoms are eliminated for clarity. The dominant α and β densities are indicated by orange and purple colors, respectively

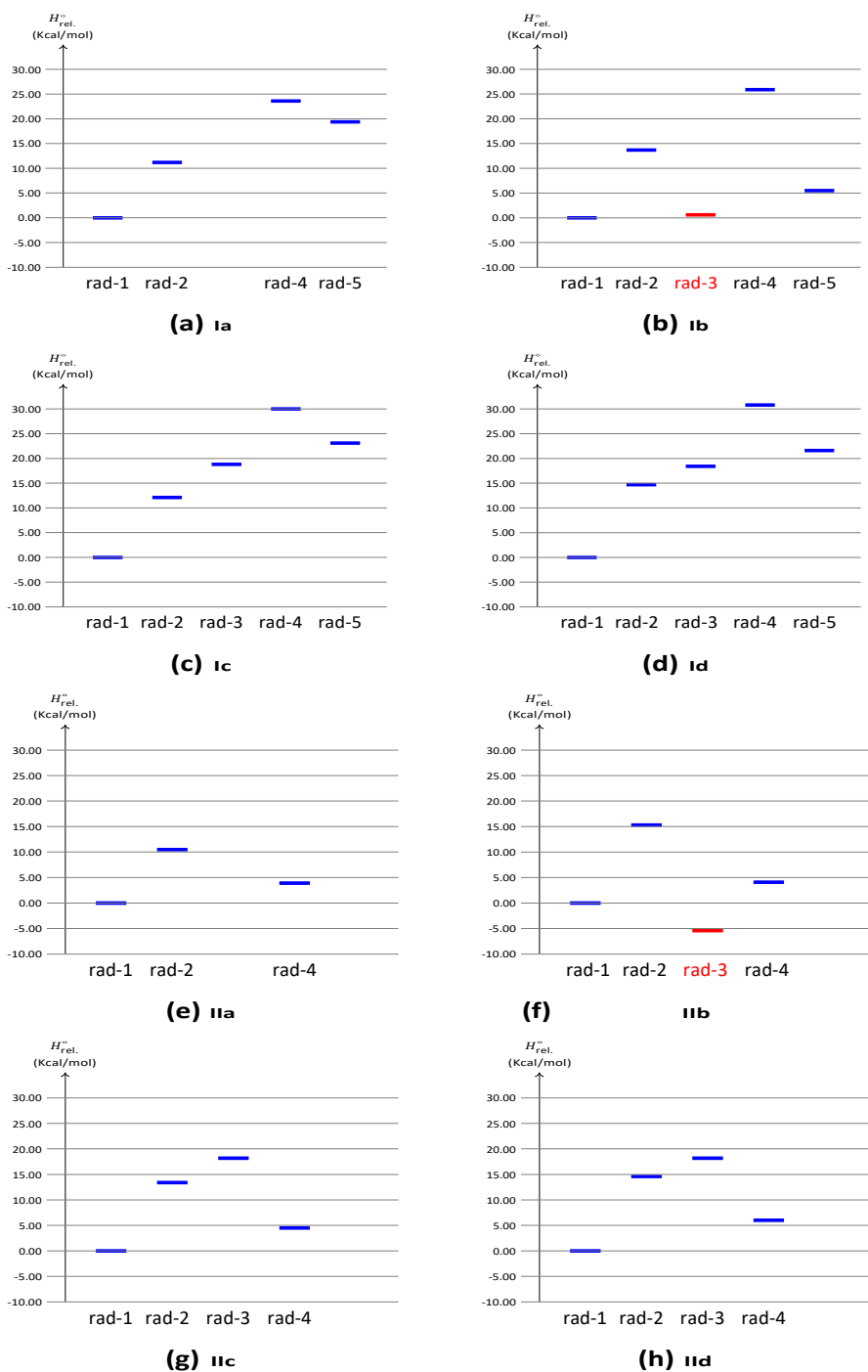


Figure S3. Stability of radicals based on standard enthalpy (H°). Radicals resulting from dissociation at site 1 and 2 are denoted as rad-1 and rad-2, respectively, and so on. The standard enthalpy of rad-1 is used as the reference value. Highly stable radicals are shown in red.

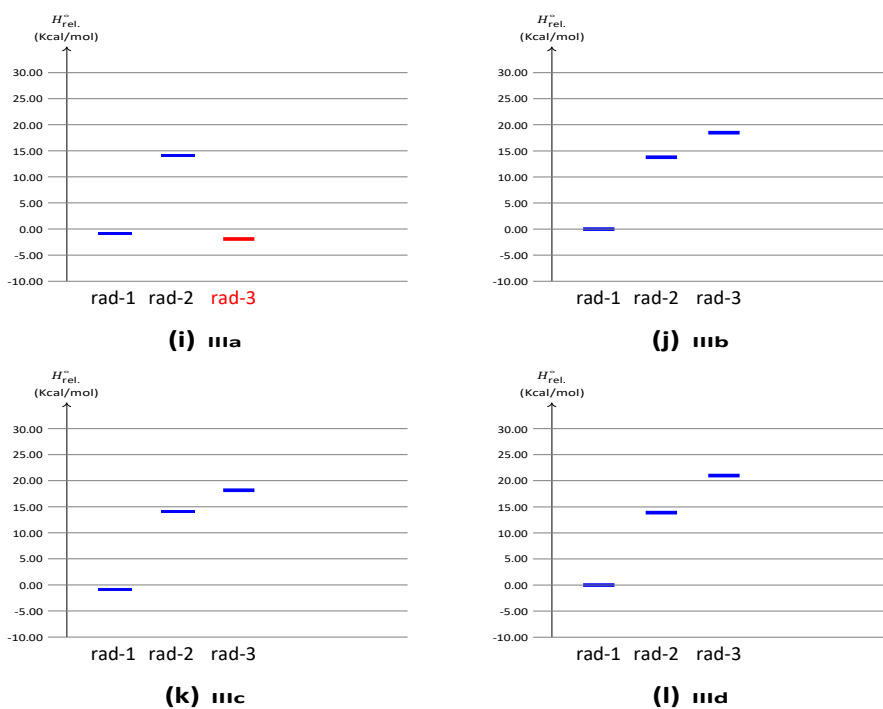


Figure S3. Stability of radicals based on standard enthalpy (H°). Radicals resulting from dissociation at site 1 and 2 are denoted as rad-1 and rad-2, respectively, and so on. The standard enthalpy of rad-1 is used as the reference value. Highly stable radicals are shown in red (continued).

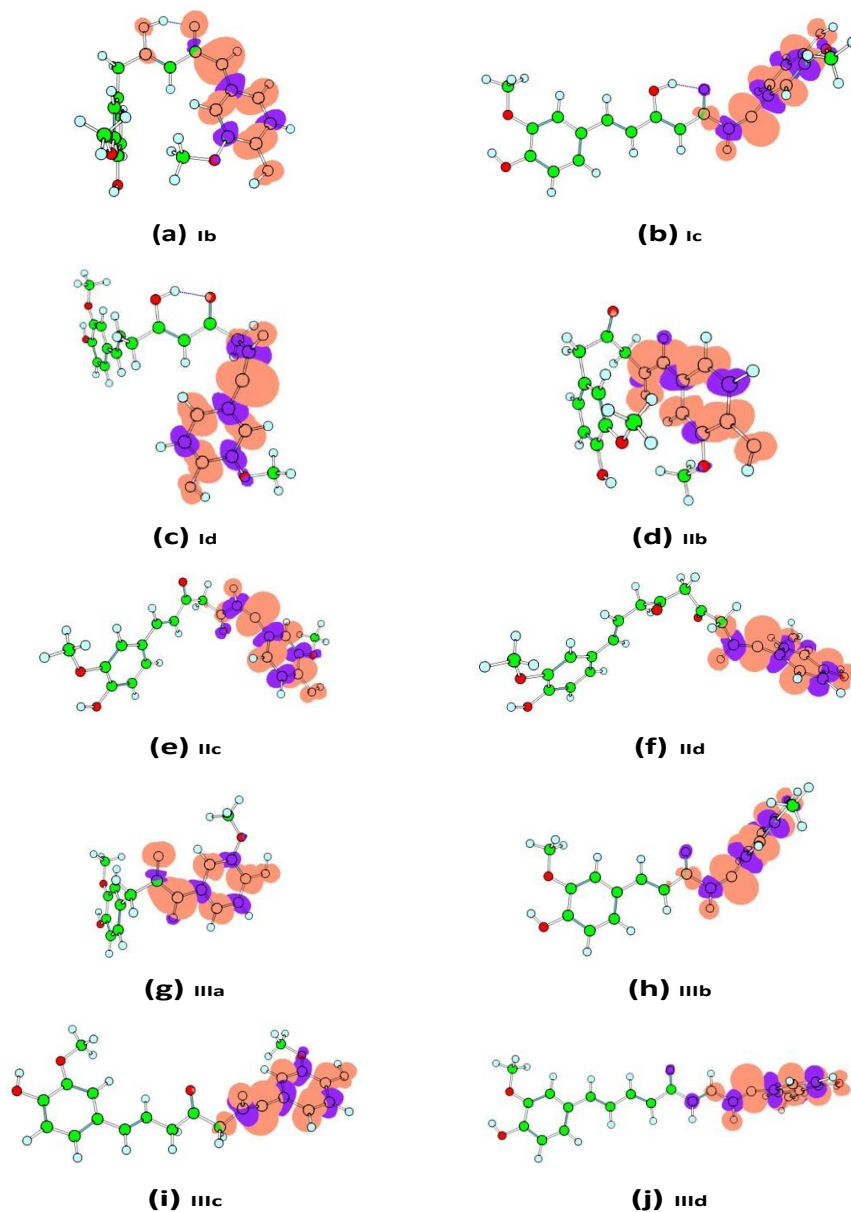


Figure S4. Spin density of radicals with isosurface of 0.002. The radicals are generated from the dissociation of site 3 (C-H bond in the linker). The dominant α and β densities are marked in orange and purple, respectively.

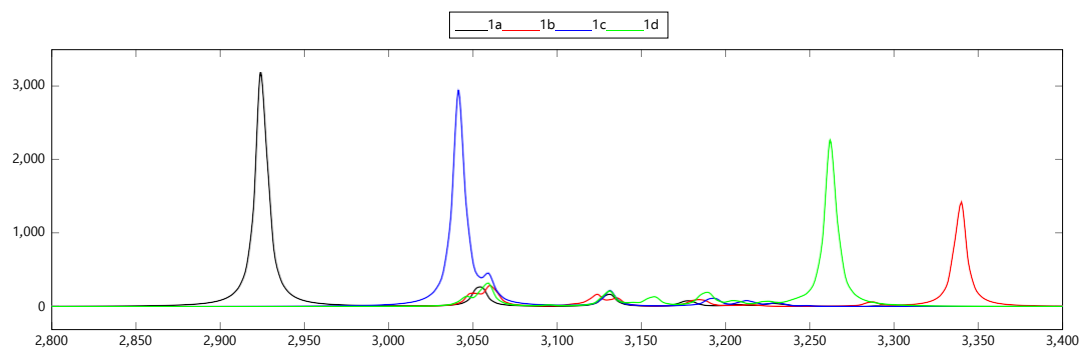
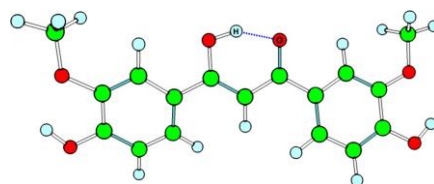


Figure S5. Infrared spectrum of members of series I, showing the peak for the stretching of the O-H bond in the enol moiety. The frequency (x-axis) is in $1/\text{cm}$ and the intensity (y-axis) is in km/mol .

Table S6. The bonding orbitals of the C-H bond (site 3) and O-H bond (site 5) as a linear combination of atomic orbitals $aX(sp^\lambda)$ and $bH(sp^0)$. X are C or O atoms. The highlighted cells represent λ values greater than three.

No.	Molecule	n	a	λ	b
Site 3 (C-H)					
1.	Ib	5	0.788	3.45	0.616
2.	Ic	7	0.777	2.67	0.629
3.	Id	9	0.777	2.72	0.630
4.	IIb	5	0.787	3.28	0.617
5.	IIc	7	0.782	2.69	0.623
6.	IIId	9	0.777	2.72	0.629
7.	IIIa	3	0.786	3.34	0.618
8.	IIIb	5	0.777	2.69	0.630
9.	IIIc	7	0.777	2.72	0.630
10.	IIId	9	0.778	2.69	0.628
Site 5 (O-H)					
11.	Ia	3	0.891	2.93	0.453
12.	Ib	5	0.884	3.10	0.467
13.	Ic	7	0.889	2.94	0.458
14.	Id	9	0.886	3.02	0.464

Table S7. Geometrical parameters of oxygen and hydrogen atoms in the moiety of Series I. The figure shows the optimized geometry of **Ia**, calculated using M06-2X.



Molecule	n	NBO Charge (e)		R: H...O	A: O-H...O
		H	O	(\AA)	(degree)
Ia	3	0.518	-0.703	1.55	150.8
Ib	5	0.522	-0.690	1.74	145.8
Ic	7	0.520	-0.720	1.60	150.0
Id	9	0.521	-0.680	1.68	146.8

Table S8. Enthalpy (kcal/mol) and entropy (cal/mol.K) of reactions via site 1 (phenolic O-H bond) and site 3 (C H-bond in the linker) of the three series

Molecules	<i>n</i>	Site 1		Site 3	
		<i>H</i>	<i>S</i>	<i>H</i>	<i>S</i>
Ia	3	2.81	0.37		
Ib	5	-0.34	3.60	0.27	8.77
Ic	7	-0.36	3.63	18.49	3.69
Id	9	-1.38	11.05	17.04	10.93
IIa	3	3.43	2.41		
IIb	5	1.09	4.43	-4.28	6.96
IIc	7	0.10	4.76	18.34	6.48
IId	9	-1.21	-5.24	16.96	0.72
IIIa	3	0.51	3.90	-1.40	10.73
IIIb	5	-0.34	3.86	18.14	5.19
IIIc	7	-1.45	5.46	16.79	4.75
IIId	9	-2.23	-3.45	18.77	4.82

References

- [1] Palash Sanphui, N. Rajesh Goud, U. B. Rao Khandavilli, Sreenu Bhanoth, and Ashwini Nangia. (2011). New polymorphs of curcumin. *Chem. Commun.* 47(2011), 5013–5015. DOI: 10.1039/c1cc10204d.